ELSEVIER

Journal of Molecular Catalysis A: Chemical 106 (1996) 267–276

JOURNAL OF MOLECULAR CATALYSIS A: CHEMICAL

Synthesis, characterization and photocatalytic properties of iron-doped titania semiconductors prepared from TiO_2 and iron(III) acetylacetonate

José A. Navío [a], Gerardo Colón [a], Marta I. Litter [b,*], Gladi N. Bianco [c]

[a] *Instituto de Ciencias de Materiales, CSIC / Dpto. de Química Inorgánica, Facultad de Química, Universidad de Sevilla, 41012-Sevilla, Spain*

[b] *Departamento Química de Reactores, Comisión Nacional de Energía Atómica, Av. del Libertador 8250, 1429 Buenos Aires, Argentina*

[c] *Departamento Química Analítica, Comisión Nacional de Energía Atómica, Av. del Libertador 8250, 1429 Buenos Aires, Argentina*

Received 6 June 1995; accepted 25 September 1995

Abstract

Specimens of iron-doped titania containing different amounts of Fe (0.5–5%) were prepared from TiO_2 (Degussa P-25) and Fe(III) acetylacetonate by the wet impregnation method. Samples were characterized by X-ray diffraction analysis, specific surface area (BET) measurements, SEM-EDX, atomic absorption and IR and diffuse reflectance spectra. From the structural point of view, the samples were similar to those obtained with $Fe(NO_3)_3 \cdot 9H_2O$ as the precursor, but with a more homogeneous distribution of iron for each mixed oxide sample on the particle surfaces but not between particles. The photocatalytic activity of these samples under near-UV irradiation was better for oxalic acid degradation than for EDTA, and similar for both types of mixed oxide samples. Mixed oxides showed however lower activity than TiO_2. Some photodegradation under visible irradiation, not occurring with TiO_2, could be observed for oxalic acid when using 5% Fe-containing samples.

Keywords: Acetylacetonate; EDTA; Iron; Oxalic acid; Oxidation; Photocatalysis; Titania

1. Introduction

The search for new materials in heterogeneous photocatalysis has been a matter of interest in the last years because of the enormous technological implications of these processes. In this sense, several studies with metal transition doped-titania have been done in recent years [1,2], related to the spectroscopic and structural properties as well to the photocatalytic behavior of these materials; however, no direct correlation between photophysical measurements and photochemical activity could be found. In particular, iron(III)-doped TiO_2 samples have been the object of several papers, including preparation and characterization, spectroscopic features, dynamics of charge-transfer trapping and recombination and photocatalytic behavior [3–32].

Our previous papers [22,30] report the preparation, characterization and some photocatalytic studies with iron-doped titania samples prepared

* Corresponding author.

SSDI 1381-1169(95)00264-2

from TiO_2 and $Fe(NO_3)_3 \cdot 9H_2O$ as iron precursor. The samples consisted of fine particles and larger aggregates with a very large distribution of particle shapes and dimensions containing non-uniformly distributed iron. Samples with high Fe contents (> 1%) contained also separate α-Fe_2O_3 or Fe_2TiO_5 phases. All samples exhibited larger particle sizes and smaller specific surface areas than the TiO_2 precursor, a lower content of surface OH groups and a smaller anatase-to-rutile ratio. Concerning their photoactivity for the oxidative degradation of oligocarboxylic acids (EDTA, oxalic and malonic acid), they presented poorer properties than naked TiO_2 (Degussa P-25), which was attributed to an enhanced recombination rate of electrons and holes and to the existence of hematite or pseudobrookite as separated phases.

In the present work, new samples of iron-doped titania were prepared by wet impregnation starting with TiO_2 and iron(III) acetylacetonate complex, $Fe(acac)_3$. The new materials were characterized by different techniques, and their photocatalytic activity for the degradation of oligocarboxylic acids under UV and visible illumination was tested.

2. Experimental

TiO_2 (Degussa P-25) was a commercial sample, gently provided by the manufacturers (Degussa, Germany) and used as provided.

Iron-doped titania powders were prepared from the iron acetylacetonate complex, $Fe(acac)_3$ (Aldrich) and P-25. Acetone solutions of $Fe(acac)_3$ containing different nominal concentrations of iron were added to TiO_2 at room temperature (Fe/TiO_2 ratios ranging from 0.5 to 5 wt.%). While the mixture was carefully stirred, the solvent was slowly evaporated. After total evaporation, the samples (named hereafter Fe/Ti(a)) were dried at 383 K for 24 h, and fired in air at 773 K for 24 h. For comparison, a sample of P-25 was also fired in air at 773 K for 24 h (named hereafter th.-pr. TiO_2, i.e., thermal-pretreated TiO_2). A sample of α-Fe_2O_3 was prepared from $Fe(acac)_3$ by thermal decomposition in air at 773 K for 24 h.

The Fe/Ti(a) oxide samples were characterized by several techniques. IR spectra were taken on a Perkin Elmer model 883 spectrophotometer using KBr pellets. X-ray diffraction (XRD) patterns of the samples were obtained at room temperature with a Philips PW 1060 diffractometer using Ni-filtered CuKα radiation. Specific surface areas (SBET) were obtained with an automatic system (Micromeritics 2200 A) with nitrogen gas as adsorbate at the liquid nitrogen temperature. Scanning electron microscopy (SEM) was performed on gold-coated samples using a JEOL apparatus, model JSM-5400 equipped with a Link analyzer model ISIS for energy-dispersive spectroscopy (EDX). UV–visible absorption spectra were obtained on a Shimadzu 210A spectrophotometer. An integrating sphere was used for diffuse reflectance spectra (DRS), using MgO as the reference. A Perkin Elmer model 2380 spectrometer was used to determine the iron content by atomic absorption. Table 1 shows the properties of all the oxide samples.

Na_2EDTA (Schuchardt) and oxalic acid (Riedel–De Haen) were of quality grade and

Table 1
Properties of the oxide samples

Type of oxide	Specific surface area ($m^2\ g^{-1}$)	Particle size (μm) [a]	X_a
TiO_2 (P-25)	49.0	0.03 [b]	0.773
TiO_2 (th.-pr.)	46.5	0.5–1	0.543
0.5% Fe/Ti (a)	44.0	1–10	0.462
0.5% Fe/Ti (n)	29.5	5 [c] + 50 [d]	0.442
1% Fe/Ti (a)	46.3	1–10	0.463
2% Fe/Ti (a)	43.8	1–10	0.464
3% Fe/Ti (a)	41.6	1–10	0.467 [e]
5% Fe/Ti (a)	41.8	1–10	0.472 [e]
5% Fe/Ti (n)	29.2	5 [c] + 180 [d]	0.452 [f]

[a] Measured by SEM.
[b] Provided by the manufacturers.
[c] Pure TiO_2.
[d] Aggregates containing Fe.
[e] Hematite peak observed.
[f] Pseudobrookite peak observed.

used as provided. Water was bidistilled in a quartz apparatus. All other reagents were of analytical grade, and used without further purification. Dilute $HClO_4$ or NaOH were used for pH adjustments.

Irradiations in the near-UV (300–400 nm) or visible range ($\lambda > 420$ nm) were performed using a high-pressure xenon arc lamp (Osram XBO, 450 W) with a 50 mm water filter to minimize IR irradiation. For near-UV irradiations, a bandpass filter (Schott Catalog No. UG1, thickness 3 mm; 300 nm $< \lambda <$ 400 nm; maximum transmission (55%) at 360 nm). Visible irradiations were performed using a cutoff filter (Schott Catalog No. GG420, thickness 2 mm).

For actinometry in the near-UV region, the ferrioxalate method [33] was used. A photon flux of 1.2×10^{-5} einstein s^{-1} dm^{-3} was calculated. Reinecke's salt actinometry [34] was used for the visible range. Approximate photon flux values were obtained taking average actinometer quantum yields. The calculated photon flux was 2.89×10^{-4} einstein s^{-1} dm^{-3}.

Photodegradations were carried out using the Fe/Ti(a) oxides obtained here and comparing the results with those of TiO_2 and the samples prepared using $Fe(NO_3)_3 \cdot 9H_2O$ as the precursor [22] (named hereafter Fe/Ti(n)). Typically, each oxide sample was suspended (0.5 g dm^{-3}) in a fresh aqueous solution of the corresponding organic acid (5×10^{-3} mol dm^{-3}) previously adjusted to pH 3; the oxide concentration guaranteed total absorption of light for all the oxide samples in the near-UV range. The suspension was ultrasonicated for 30 s, and a sample of 2 ml was irradiated at 298 K in a thermostatted quartz cell (10 mm pathlength) for 2 h with magnetic stirring. A water-saturated oxygen stream was bubbled in the suspension at a constant rate of 30 ml/min throughout the experiment. After irradiation, the suspension was filtered through a Millipore (0.2 μm) membrane. The photodegradation of the organic acid was evaluated by determining its concentration before and after the irradiation by comparison with a blank in the dark. Irradiations of the organic acids in the absence of catalyst were also performed in the same conditions. At least three experiments were carried out for each condition, averaging the results.

A Varian 5000 high performance liquid chromatograph, equipped with a conductimetric Milton Roy ConductoMonitor III detector, with electronic conductivity suppressor and a Spectra Physics 4290 integrator, was used to determine oxalic acid concentrations. The following conditions were used: Wescan Anion 269-0001 column (anion interchange); eluant, 2 g dm^{-3} Na_2EDTA; flow rate, 1.5 ml/min; 100 μl loop [1]. Fresh standards were used daily for calibration curves. This method allowed determinations with less than 5% error.

EDTA determination was carried out by spectrophotometric analysis of the Co(II) complex [35]. In the range of concentrations used, EDTA could be determined with an error of 8%. For Fe/Ti oxides, total iron in solution was determined by the thioglycolate method [36]. In all spectrophotometric techniques calibration curves were obtained first.

3. Results and discussion

3.1. Characteristics of the catalysts

In Table 1 the main characteristics of all the oxide samples are listed. Bulk and surface characterization of the mixed Fe/Ti(n) samples can be found elsewhere [22].

Regarding the BET surface areas of the samples, it can be inferred that the incorporation of different amounts of iron into TiO_2 by the procedure described above, does not lead to any considerable differences in the SBET values of these samples. On the contrary, Fe/Ti(n) samples yielded much lower SBET values. This

[1] Method recommended by Wescan Instrument, Inc. in *The Wescan Ion Analyzer*, 7 (1984) 3.

result clearly indicates that the nature and size of the precursor can also have influence on the texture of the processed samples, i.e., a voluminous precursor such as $Fe(acac)_3$ could not penetrate the microporous surface of the support thereby not reducing the surface area. Comparing all samples with original (not calcined) P-25, it can be concluded that the slight reduction on area is due exclusively to the thermal treatment (cf. P-25 with th.-pr. TiO_2).

SEM studies showed that whereas th.-pr. TiO_2 consists of fine round particles of 0.5–1 μm, Fe/Ti(a) oxide samples showed similar shapes with a particle size distribution of 1–10 μm in all the samples. EDX analysis showed that, although in all Fe/Ti(a) samples the semiquantitative acquisition gave mean iron contents close to the nominal ones, spot EDX analysis revealed a non-uniform distribution of iron but only between particles. However, a homogeneous distribution of iron was always found on the particle surface, although these iron contents were generally different than the corresponding nominal ones. The almost complete homogeneity in shape and size distributions (1–10 μm) observed for Fe/Ti(a) samples contrasts strongly with the very large distribution of shapes and dimensions (50 μm and 180 μm), containing non-uniformly distributed iron, observed for Fe/Ti oxides prepared from iron nitrate. These results suggest that, although the wet impregnation method does not seem to be a suitable procedure to obtain a uniform distribution of the dopant (Fe^{3+}) into the matrix oxide, the use of $Fe(acac)_3$ instead of $Fe(NO_3)_3.9H_2O$ as the precursor yields a more homogeneous distribution of iron for each mixed oxide sample on the particle surfaces but not between particles. This is probably due to the fact that deposition of iron takes place by reaction of the corresponding acac complex with the surface hydroxyl groups of the support, according to Eq. 1:

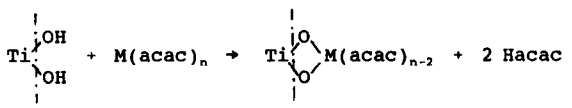

(1)

leading to a well-dispersed supported Fe/Ti

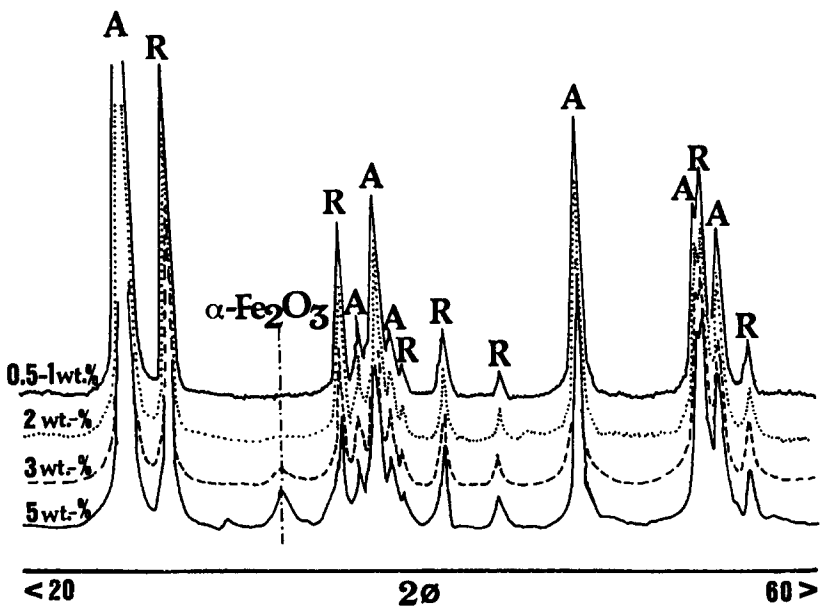

Fig. 1. XRD patterns of selected iron-doped titania samples, with the indicated nominal contents of Fe^{3+}. A = anatase and R = rutile peaks.

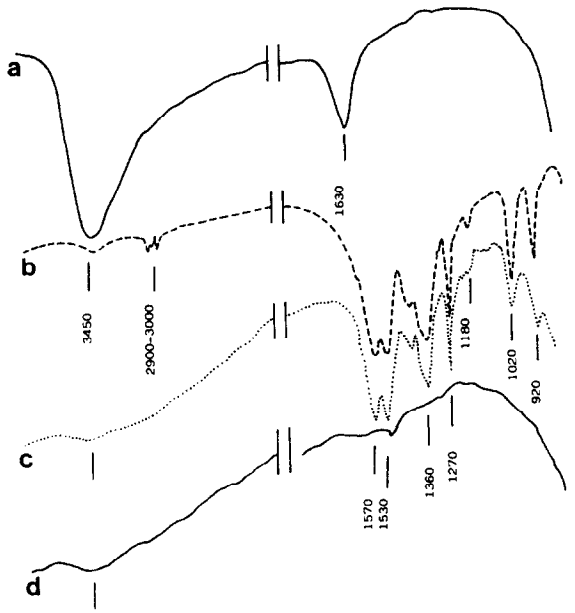

Fig. 2. IR spectra of oxide samples: (a) th.-pr. TiO_2; (b) $Fe(acac)_3$ complex; (c) $Fe(acac)_3/TiO_2$ precursor (before thermal treatment); (d) Fe/Ti(a) sample after heating in air. Similar spectra are obtained for the iron-treated titania samples, independently of the iron content.

oxides, as observed in other metal/TiO_2 catalysts [37,38].

In Fig. 1 we show the XRD patterns of selected iron-doped titania samples. The molar fraction of anatase (X_A) was calculated according to the method described elsewhere [39]. From the analysis of XRD results for the Fe/Ti(a) samples, it can be concluded that A/R ratios are lower than that of TiO_2 in its calcined or original form and practically the same in all the doped samples. This indicates that starting TiO_2 matrix is altered by the presence of iron, but this alteration seems to be independent of the nominal concentration of iron. In addition, samples with 3–5 wt.% Fe showed also α-Fe_2O_3 (hematite) peaks as a separate phase. As previously reported [22], Fe/Ti(n) oxides present similar A/R ratios, with the 5 wt.% Fe sample showing X-ray peaks assigned to pseudobrookite (Fe_2TiO_5). From the structural point of view, the present results are not very different from the mixed oxides obtained from iron nitrate.

3.2. Infrared spectra

In Fig. 2 are shown the IR spectra of th.-pr. TiO_2 (a), $Fe(acac)_3$ complex (b), $Fe(acac)_3/TiO_2$ precursor (before thermal treatment) (c) and an Fe/Ti(a) sample after heating in air (d). Spectrum of the original TiO_2 surface (a) showed a broad band centered at 3450 cm^{-1}, ascribed to basic hydroxyl groups [40,41], whereas a band at 1630 cm^{-1} corresponds to adsorbed molecular water. These results clearly

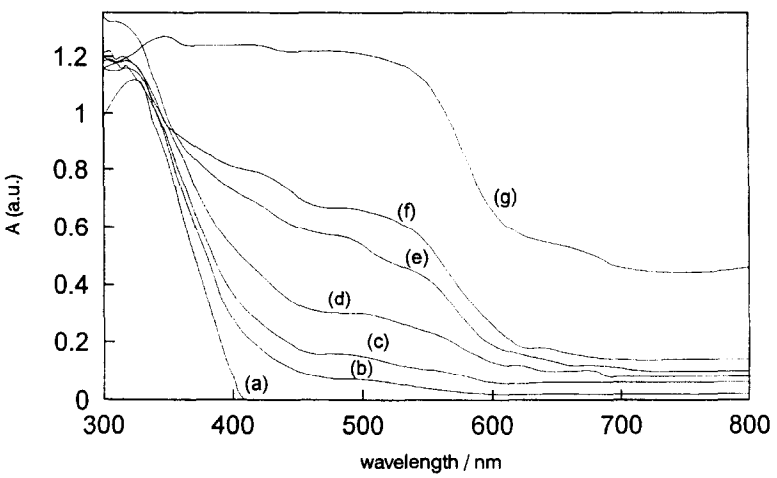

Fig. 3. DRS (vs. MgO) of oxide samples: (a) TiO_2 (Degussa P-25); (b) 0.5 wt.% Fe/Ti(a); (c) 1 wt.% Fe/Ti(a); (d) 2 wt.% Fe/Ti(a); (e) 3 wt.% Fe/Ti(a); (f) 5 wt.% Fe/Ti(a); (g) α-Fe_2O_3 prepared from $Fe(acac)_3$.

indicate that the original P-25 surface is hydrated and hydroxylated. Comparison of spectra (b) and (c) shows that the character of the acetylacetonate ligand is still present after the metal complex have been attached (cf. bands at 1570, 1530, 1390 and 1270 cm^{-1} [42]). However, after the attachment of the iron complex onto the TiO_2 surface, the band at 3450 cm^{-1} almost disappears, providing unequivocal evidence that $Fe(acac)_3$ has been attached to the TiO_2 surface by reaction with the surface hydroxyl groups of the oxide (Eq. 1), as previously proposed for other metal/TiO_2 catalysts [38].

In addition, IR results point out that the surface of the Fe/Ti catalysts prepared by this method seems to be almost dehydrated/dehydroxylated (spectrum d). These results suggest that although this preparation method gives a well dispersed Fe^{3+} on the support, the degree of dehydroxylation could forecast a loss of photoactivity on these iron-doped titania catalysts in comparison with that expected for pure TiO_2.

3.3. Diffuse reflectance spectra

DRS of Fe/Ti(a) samples in comparison with TiO_2 and α-Fe_2O_3 prepared from $Fe(acac)_3$ are depicted in Fig. 3. As it is known [31,43], TiO_2 (Degussa P-25) shows an absorption threshold at 408 nm (3.04 eV) and an $O^{2-} \rightarrow Ti^{4+}$ charge-transfer band with a maximum at 325 nm. The spectral characteristics of Fe/Ti samples prepared from iron nitrate are reported elsewhere [22]. Diffuse reflectance spectra of these samples were not well-resolved, indicating a large dispersion and disorder of Fe^{3+} species in the TiO_2 lattice and surface. The spectra of the Fe/Ti(n) oxide samples resembled that of TiO_2 with the onset shifted towards the visible (450 nm for the 0.5 wt.% Fe/TiO_2 sample and 500 nm for the 5 wt.% Fe/TiO_2 sample); in the 5 wt.% Fe sample some features indicated the presence of small amounts of Fe_2O_3 or Fe_2TiO_5. On the contrary, the new Fe/Ti oxide samples prepared from acac exhibit more structured spectra. All samples show enhanced absorptions in the range 400–650 nm, increasingly higher for the more iron-charged samples and accompanying the changes on color from pale yellow to reddish brown. Samples containing 0.5 to 1 wt.% Fe (b,c) show spectra similar to TiO_2 but with a constant absorption in the visible region higher than that of P-25. Also, the onset of the absorption is shifted to the red. In samples with a higher iron content (d–f), a broad band centered at ca. 500 nm can be seen, the spectra becoming increasingly similar to that of α-Fe_2O_3. In all Fe/Ti(a) samples the $O^{2-} \rightarrow Ti^{4+}$ charge-transfer band can be observed at ca. 320 nm.

The red shift of the absorption edge of Fe(III) doped-titania has been attributed to the excitation of 3d electrons of Fe^{3+} to the TiO_2 conduction band (charge-transfer transition) [12], according to the energy levels proposed [3]. The broad band centered at 500 nm, which exhibits an approximately linear increase with iron content, can be ascribed to the d–d transition $^2T_{2g} \rightarrow {}^2A_{2g}, {}^2T_{1g}$ or to charge-transfer transitions between dopant ions via the conduction band ($Fe^{3+} + Fe^{3+} \rightarrow Fe^{4+} + Fe^{2+}$). The increased absorption in the visible can be due also to transitions implicating surface states or native defects in the lattice [3].

3.4. Photocatalytic degradation of oligocarboxylic acids

Neither oxalic acid nor EDTA were degraded under irradiation (near-UV or visible light) in the absence of catalyst in the present conditions, as it was found in our previous work [30].

Figs. 4 and 5 show the results of photodegradation of oxalic acid and EDTA (pH 3) in the presence of 0.5 g dm^{-3} catalyst after 2 h near-UV irradiation (300 nm $< \lambda <$ 400 nm). In separated experiments in the dark, the amount of substrate (EDTA or oxalic acid) adsorbed on the catalyst surface was determined. It was found that it was always less than the detection limit and therefore, no corrections for adsorption were

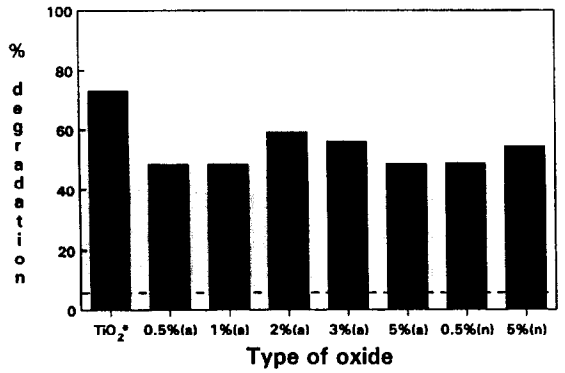

Fig. 4. Photodegradation of oxalic acid in O_2-saturated aqueous suspension under near-UV irradiation (300 nm $< \lambda <$ 400 nm); [catalyst] = 0.5 g dm^{-3}, [oxalic acid] = 5×10^{-3} mol dm^{-3}, pH 3, T = 298 K, irradiation time = 2 h.
* Degussa P-25 not calcined.

made. Broken lines in the figures represent the experimental limit of detection.

It can be seen that all oxide samples are effective catalysts. This is not in contradiction with our earlier results [30], that showed no reactivity for EDTA degradation with Fe/Ti(n) samples and a lower degradation of EDTA with TiO_2, because photodegradation in the 300–400 nm region is quite dependent on the spectrum of the excitation light. As found previously by us for these oligocarboxylic acids [30] and by others for substrates such as phenols or alcohols [14,21,25,26,28], TiO_2 P-25 (not calcined) is

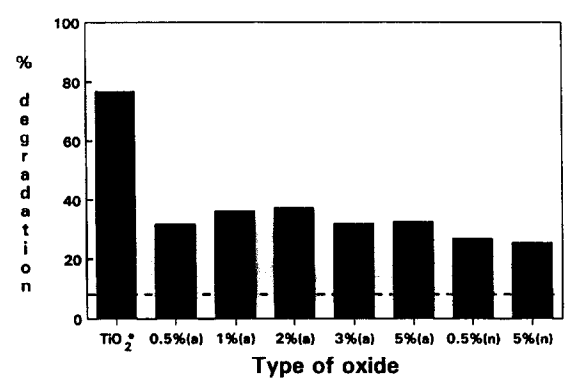

Fig. 5. Photodegradation of EDTA in O_2-saturated aqueous suspension under near-UV irradiation (300 nm $< \lambda <$ 400 nm); [catalyst] = 0.5 g dm^{-3}, [EDTA] = 5×10^{-3} mol dm^{-3}, pH 3, T = 298 K, irradiation time = 2 h.
* Degussa P-25 not calcined.

Table 2
Degradation of oxalic acid (5×10^{-3} mol dm^{-3}) under visible irradiation ($\lambda > 420$ nm) in the presence of 1 g dm^{-3} catalyst; irradiation time = 3 h

Type of oxide	% degradation (dark)	% degradation (visible) [a]
TiO_2 (P-25)	[b]	5.4
0.5 wt.% Fe/Ti (n)	[b]	8.0
0.5 wt.% Fe/Ti (a)	5.4	11.3(6.2)
5 wt.% Fe/Ti (n)	9.6	17.9(10.7)
5. wt.% Fe/Ti (a)	7.5	11.1(7.1)

[a] In parentheses, net degradation due to irradiation.
[b] Negligible.

the most efficient material. In the present case, the degree of degradation with TiO_2 was approximately the same for both substrates (ca. 75%). Doped oxides gave lower degrees and were more efficient to degrade oxalic acid than EDTA. Although it is very difficult to discern differences in activity between the mixed oxides in function of the iron content, the efficiency seems to be at its maximum for the 2% iron sample.

No photocatalytic degradation was found under visible irradiation ($\lambda > 420$ nm) in the above conditions (0.5 g dm^{-3} of catalyst, 2 h irradiation), but some degradation of oxalic acid was observed with Fe-containing samples (especially with the 5 wt.% Fe/Ti samples) when doubling the oxide concentration and increasing the irradiation time to 3 h. Results are shown in Table 2. In these conditions, due to a higher extent of adsorption, dark reactions were not negligible, but the loss of oxalic acid was always higher under irradiation. On the contrary, no photodegradation of EDTA was observed in the same conditions.

Photocorrosion of mixed oxides was evaluated only for the samples containing 5% iron, measuring the amount of total iron released in solution (dark reaction not discounted). Samples with a lower iron content gave erratic results. The results (Table 3) indicate that samples prepared from acac are less stable than Fe/Ti(n) samples, the corrosion reaching in some cases

Table 3
Extent of iron dissolution in selected photocatalytic experiments

Substrate	Wavelength range	Per cent dissolution	
		5% Fe/Ti (n)	5% Fe/Ti (a)
oxalic acid	near-UV	6.7	15.8
oxalic acid	visible	5.7	10.2
EDTA	near-UV	6.2	11.8

Conditions are those of Figs. 4 and 5, and Table 2

more than 15%. Also, dissolution was more extensive under UV illumination.

As it is well known, photocatalytic oxidative degradations involve the production of e^-/h^+ pairs by semiconductor (SC) irradiation:

$$SC \xrightarrow[E>E_g]{h\nu} e^-_{cb} + h^+_{vb} \quad (2)$$

The reaction of these entities with species present in solution gives rise to redox reactions. The occurrence of different reactions depends on the electrochemical potentials of the species in solution and the redox levels of the valence and conduction bandedges of the semiconductors. The presence of oxygen is necessary to enhance separation of photoproduced electrons and holes and, when iron is present, is important to prevent photocorrosion by competition for the conduction-band electrons [44–48]:

$$O_2 \xrightarrow{e^-_{cb}} O_2^{\cdot-} \rightarrow \rightarrow H_2O_2 \rightarrow \rightarrow OH^{\cdot} \quad (3)$$

On the other hand, an oxidizable substrate (S) can be attacked directly by holes or can react with $OH^{\cdot}$ formed on the semiconductor surface:

$$S + h^+ \rightarrow S_{ox} \quad (4)$$

$$S + OH^{\cdot} \rightarrow S_{ox} \quad (5)$$

Photocatalysis with TiO_2 is only possible with UV light ($\lambda < 400$ nm). The same energy restriction holds for mixed Ti/Fe catalysts, because photogeneration of e^-/h^+ pairs from TiO_2 is not (or only marginally) affected by Fe^{3+} [7]. It has been proved that no visible-light sensitized photoconductivity exists for iron-doped titania samples, which excludes the possibility of photogeneration of e^-/h^+ pairs at these wavelengths [1].

Working with Fe/Ti Q-sized oxides, it was found that lifetimes of electrons and holes are enhanced in comparison with pure TiO_2 due to electron or hole trapping at Fe(III) centers [12,16], this fact favoring redox processes. Higher photocatalytic activities with mixed oxides are indeed found in photooxidations, but only with these Q-sized particles (diameter < 10 nm) [2,24]. However, when these particles were heated, they agglomerated decreasing the possibility of trapping, not only due to a decrease of surface area but because dopants are isolated far from the surface and the transfer of trapped charge carriers to the interface is reduced [2]. Actually, a lower reactivity was found in our case even with Fe/Ti(a) in which iron is homogeneously distributed onto the TiO_2 surface. Similar results have been obtained by Serpone et al. with colloidal particles (ca. 13 nm) containing 10 wt.% Fe. This reduced activity can be explained because dopants act more as recombination centers than as trap sites for charge transfer at the interface. As we mentioned in our previous paper [30], due to the presence of a second phase (iron oxide and/or pseudobrookite) the system behaves as in the case of 'coupled semiconductors', with holes located at the less oxidizing level corresponding to pure iron oxide (*ca.* + 2.44 V at pH 3 compared with + 3.19 V for TiO_2). Bickley et al. arrived at similar conclusions [31], and this can explain the observed trend in catalytic activity, slightly increasing up to 2% iron-containing samples (where the second phase cannot be detected by XRD) and then decreasing. In addition, an enhanced recombination is possible due to the rather low mobility of photoexcited electrons in these iron oxide or mixed phases.

Differences in photoactivity between TiO_2 and mixed oxides can be also attributed to other characteristics such as the larger particle size and the lower (A/R) ratio in the Fe/Ti oxide samples. Also, the lower amount of OH surface groups, proved in the present case by IR spec-

troscopy, can cause a lower adsorption of the substrate. In fact, the role of surface hydroxyl groups in controlling the photoactivity of powdered TiO_2 specimens has been widely recognized [26,49]. Some inactivation of the samples by photocorrosion may also contribute, specially in Fe/Ti(a) samples, which seems to be more photocorrodible than Fe/Ti(n) samples. In addition, EDX results evidenced the presence of rests of charcoal arising from the thermal decomposition of the acetylacetonate during the firing process; this could also influence negatively the photoactivity of Fe/Ti samples prepared by this technique.

The higher photocorrosion of Fe/Ti(a) samples can be tentatively explained taking in account that the preparation technique gives rise to a more homogeneous distribution of Fe^{3+} on the surface, which can scavenge photoelectrons rapidly to form Fe^{2+}, whereas in nitrate-based samples electrons must diffuse through iron oxide deposits of lower conductivity.

The fact that oxalic acid is more easily degraded than EDTA in the near-UV range by mixed oxides can be attributed to the existence of other possible pathways such as photolysis of surface or homogeneous complexes (photofenton-type reaction), the last generated by dissolved iron; both processes give rise to ligand degradation. As we cited in our previous paper [30], the Fe(III)–oxalato complex absorbs in the range 240–475 nm and gives a photolysis quantum yield close to the unity all over this range, whereas the Fe(III)–EDTA complex only absorbs at $\lambda < 400$ nm with a much lower ϕ value. Therefore, it is clear that the photolysis of oxalato-complexes can make an important contribution under UV illumination, promoting ligand oxidation even with visible light. This explains the small but detectable degradation of oxalic acid under visible irradiation with a more concentrated suspension of Fe/Ti catalyst, more extensive in the case of 5% Fe samples. The absence of photoconductivity of Fe/Ti samples [1] under visible light clearly supports that the only possibility for photoreaction at these longer wavelengths is through homogeneous or heterogeneous charge-transfer reactions involving Fe(III)–complexes. Sclafani et al. [26] also emphasize the importance of these processes.

4. Conclusions

Fe/Ti oxide samples have been prepared by a method which provides a better homogeneous distribution of iron into the TiO_2 particle keeping practically unchanged the specific surface area of the catalyst. However, their photocatalytic activity is still lower than that of pure TiO_2, as in the case of Fe/Ti oxide samples prepared from iron nitrate. Using more concentrated suspensions of the oxides, Fe/Ti catalysts can promote substrate degradation under visible light when homogeneous or heterogeneous Fe(III)–complexes, active at these wavelengths, are formed.

The preparation of mixed oxides through a sol–gel technique at room temperature can provide samples with well-dispersed iron into the TiO_2 matrix, with a higher A/R ratio and a higher surface OH content, which could be better catalysts. We shall report further on results in this direction.

Acknowledgements

To Dr. E. San Román from INQUIMAE-UBA (Argentina) for helpful discussions. To Francisco Parisi, División Física del Sólido (CNEA) for X-ray measurements. J.A.N. wish to thank 'Dirección General de Investigación Científica y Técnica (DGICYT-Spain), PB93-0917' for supporting part of this work. M.I.L. is a member from CONICET (Argentina).

References

[1] N. Serpone and D. Lawless, Langmuir, 10 (1994) 643.
[2] W. Choi, A. Termin and M.R. Hoffmann, J. Phys. Chem., 98 (1994) 13669, and references therein.

[3] K. Mizushima, M. Tanaka, A. Asai and S. Iida, J. Phys. Chem. Solids, 40 (1979) 1129.
[4] G.N. Schrauzer and T.D. Guth, J. Am. Chem. Soc., 99 (1977) 7189.
[5] M.A. Malati and W.K. Wong, Surf. Technol., 22 (1984) 305.
[6] M. Schiavello and A. Sclafani, in M. Schiavello (Ed.), Photoelectrochemistry, Photocatalysis and Photoreactors, NATO-ASI, Series C 146, D. Reidel Publish. Co., Dordrecht, 1985, p. 503.
[7] D. Cordishi, N. Burriesci, F. D'Alba, M. Petrera, G. Polizzotti and M. Schiavello, J. Solid State Chem., 56 (1985) 182.
[8] R.I. Bickley and J.A. Navío-Santos, in G. Grassi and D.O. Hall (Eds.), Photocatalytic Production of Energy-Rich Compounds, Elsevier Applied Sci., London, 1985, p. 105.
[9] S. Zielinski and A. Sobczynski, Acta Chim. Hung., 120 (1985) 229.
[10] J.G. Van Ommen, H. Bosch, P.J. Gellings and J.R.H. Ross, Stud. Surf. Sci. Catal., 31 (1987) 151.
[11] J. Soria, J.C. Conesa, V. Augugliaro, L. Palmisano, M. Schiavello and A. Sclafani, J. Phys. Chem., 95 (1991) 274.
[12] J. Moser, M. Grätzel and R. Gallay, Helv. Chim. Acta, 70 (1987) 1596.
[13] V. Augugliaro and L. Palmisano, in M. Schiavello (Ed.), Photocatalysis and Environment, Kluwer Academic Publ., Dordrecht, 1988, p. 425.
[14] L. Palmisano, V. Augugliaro, A. Sclafani and M. Schiavello, J. Phys. Chem., 92 (1988) 6710.
[15] O.A. Ileperuma, F.N.S. Weerasinghe and T.S. Lewke Bandara, Solar Energy Mater., 19 (1989), 409.
[16] J.C. Conesa, J. Soria, V. Augugliaro and L. Palmisano, Stud. Surf. Sci. Catal., 48 (1989) 307.
[17] M. Grätzel and R.F. Howe, J. Phys. Chem., 94 (1990) 2566.
[18] J.A. Navío, M. García Gómez, M.A. Pradera Adrián and J. Fuentes Mota, Stud. Surf. Sci. Catal., 59 (1991) 445.
[19] J.A. Navío, F.J. Marchena, M. Roncel and M.A. De la Rosa, J. Photochem. Photobiol. A, 55 (1991) 319.
[20] R. I. Bickley, T. González-Carreño and L. Palmisano, Mater. Chem. Phys., 29 (1991) 475.
[21] Z. Luo and Q.-H. Gao, J. Photochem. Photobiol. A, 63 (1992) 367.
[22] J.A. Navío, M. Macías, M. González-Catalán and A. Justo, J. Mater. Sci., 27 (1992) 3036.
[23] R.I. Bickley, J.S. Lees, R.J.D. Tilley, L. Palmisano and M. Schiavello, J. Chem. Soc., Faraday Trans., 88 (1992) 377.
[24] D.W. Bahnemann, Isr. J. Chem., 33 (1993) 115.
[25] R.I. Bickley, L. Palmisano, M. Schiavello and A. Sclafani,Stud. Surf. Sci. Catal., 75 (1993) 2151.
[26] A. Sclafani, L. Palmisano and M. Schiavello, Res. Chem. Intermed., 18 (1992) 211.
[27] A.B. Rives, T.S. Kulkarni and A.L. Schwaner, Langmuir, 9 (1993) 192.
[28] L. Palmisano, M. Schiavello, A. Sclafani, C. Martin, I. Martin and V. Rives, Catal. Lett., 24 (1994) 303.
[29] A. Milis, J. Peral, X. Domènech and J.A. Navío, J. Mol. Catal., 87 (1994) 67.
[30] M.I. Litter and J.A. Navío, J. Photochem. Photobiol. A, 84 (1994) 183.
[31] R. I. Bickley, T. González-Carreño, A.R. González-Elipé, G. Munuera and L. Palmisano, J. Chem. Soc., Faraday Trans., 90 (1994) 2257.
[32] S.T. Martin, H. Herrmann, W. Choi and M.R. Hoffmann, J. Chem. Soc., Faraday Trans., 90 (1994) 3315.
[33] C.G. Hatchard and C.A. Parker, Proc. Roy. Soc. A, 235 (1956) 518.
[34] E.E. Wagner and A.W. Adamson, J. Am. Chem. Soc., 88 (1966) 394.
[35] K.L.E. Kaiser, Water Res., 7 (1973) 1465.
[36] D.L. Leussing and I.M. Kolthoff, J. Am. Chem. Soc., 75 (1953) 390.
[37] P.J. van den Brink, A. Scholten, A. van Wageningen, M.D.A. Lamers, A.J. van Dillen and J.W. Geus, Stud. Surf. Sci. Catal., 63 (1991) 527.
[38] J.A. Navío, M. Macías, F.J. Marchena and C. Real, Stud. Surf. Sci. Catal., 72 (1992) 423.
[39] J.M. Criado, C. Real and J. Soria, Solid State Ionics, 32/33 (1989) 461.
[40] M. Primet, P. Pichat and M.V. Mathieu, J. Phys. Chem., 75 (1971) 1221.
[41] G. Munuera, F. Moreno and J.A. Prieto, Z. Phys. Chem., 78 (1972) 112.
[42] K. Nakamoto, in Infrared and Raman Spectra of Inorganic and Coordination Compounds, 4th. Ed., Wiley, New York 1986.
[43] R.I. Bickley, T. González-Carreño, J.S. Lees, L. Palmisano and R.J.D. Tilley, J. Solid State Chem., 92 (1991) 178.
[44] M.I. Litter and M.A. Blesa, J. Colloid Interface Sci., 125 (1988) 679.
[45] M.I. Litter and M.A. Blesa, Can. J. Chem., 68 (1990) 728.
[46] M.I. Litter, E.C. Baumgartner, G.A. Urrutia and M.A. Blesa, Environ. Sci. Technol., 25 (1991) 1907.
[47] M.I. Litter and M.A. Blesa, Can. J. Chem., 70 (1992) 2502.
[48] M.I. Litter and M.A. Blesa, Can. J. Chem., 72 (1994) 2037.
[49] J.A. Navío and V. Rives-Arnau, Langmuir, 6 (1990) 1525.